END
DATE
FILMED

8 ─ 77

DDC

Report No. 03-72-159

FIBER-OPTIC-COUPLED LOC INJECTION-LASER ARRAY
FOR 8500 Å ROOM-TEMPERATURE EMISSION

Final Report

Prepared by

David L. Carr and Friedrich H. Doerbeck

December 1972

Prepared for

Night Vision Laboratory
U. S. Army Electronics Command
Fort Belvoir, Virginia 22060

Contract No. DAAK02-72-C-0257

Texas Instruments Incorporated
Semiconductor Group
P. O. Box 5012
Dallas, Texas 75222

ADA042490

DDC
RECEIVED
AUG 5 1977
A

Report No. 03-72-159

FIBER-OPTIC-COUPLED LOC INJECTION-LASER ARRAY
FOR 8500 Å ROOM-TEMPERATURE EMISSION

Final Report

Prepared by

David L. Carr and Friedrich H. Doerbeck

December 1972

Prepared for

Night Vision Laboratory
U. S. Army Electronics Command
Fort Belvoir, Virginia 22060

Contract No. DAAK02-72-C-0257

Texas Instruments Incorporated
Semiconductor Group
P. O. Box 5012
Dallas, Texas 75222

ABSTRACT

The objective of this program was to fabricate a fiber-optic-coupled injection-laser array for the wavelength of 8500 Å at room temperature. The laser devices used are of the narrow-beam-angle large-optical-cavity (LOC) type. The array emitted 84 watts peak optical power from an emission aperture of 15 mils by 20 mils, with a peak wavelength of 8420 Å and a half-intensity beamwidth of 38°, when driven with pulses of 50-amps peak current, 150-ns duration, and 5-kHz repetition rate.

Report No. 03-72-159

TABLE OF CONTENTS

Report No. 03-72-159

LISTS OF ILLUSTRATIONS

SECTION I
INTRODUCTION

The objective of this program was to fabricate an injection-laser illuminator array emitting near-infrared radiation at a room-temperature wavelength of 8500 Å, with the individual laser diodes optically coupled by fiber-optic ribbons to a 20-mil by 20-mil emission aperture.

The fundamental task in any illuminator system is to direct sufficient power onto a given area, usually under the additional requirement to keep the collimating optics as small as possible. Therefore, the property of prime importance for the light source in such a system is radiance, measured in watt cm^{-2} steradian^{-1}.

To increase the total emitted power, laser diodes are assembled into arrays. The array normally has the same beam-angle divergence as a single device. The total power may be less than the sum of the individual diodes because of the temperature rise due to poor heat sinking, resulting from the necessity of electrical isolation for series string current driving. But the most adverse result of array fabrication is normally the increase in the area of the effective emission aperture. Several plans have been used to arrange laser diodes in proximity for minimum aperture arrays. The best stairstep arrays achieve a ratio of emitting to not-emitting area of 1/200.

The array of this program has the diodes coupled optically by the optical fiber ribbons. By the use of 1-mil by 12-mil optical fiber ribbons, the array-emission area can be reduced by seven times over that of a stairstep array with the same number of diodes. Because the emission beam angle is increased by passage through the fibers, the energy emitted into the required 45° solid-cone angle (f/1.2) is reduced $\sim$ 30 to 40%, resulting in a brightness increase in the array of $>$ 6 due to the use of the fiber optics. Additional benefits of fiber-optic coupling are better heat sinking due to diode placement independent of optical considerations and simpler array fabrication methods.

The development of two processes was required: 1) the solution epitaxial growth of efficient GaAlAs injection-laser material for emission at 8500 Å with a narrow beam angle, and 2) the technique of coupling fiber-optic ribbons to injection lasers. Originally, it had been planned to use GaAlAs single-heterostructure lasers with sufficient Al in the recombination region to reduce the emission wavelength from 9100 Å (for GaAs) to 8500 Å at 300°K. Because such lasers proved difficult to reproduce and generally degraded easily, the emphasis was shifted to the large-optical cavity (LOC) structure. The LOC is capable of high power efficiency and resistance to degradation.

1

However, in reducing the normal ~ 60° emission beam solid-angle to 45°, as required for the array, these two qualities must be compromised. LOC-lasers emitting 0.5 to 1.2 watts/mil of facet width, at a wavelength of 8420 Å, and 45° beam angle were used in the delivered array. To the best of our knowledge, this is the first fiber-optically coupled LOC laser array that has been built.

Techniques were developed for coupling 1-mil by 12-mil optical fiber ribbons to the emitting facets of LOC injection lasers, with typically 70 to 90% coupling efficiency. The ribbons were bundled at the output end so that the emission aperture was reduced to 15 mils by 20 mils.

The delivered array emitted 84 watts maximum peak optical power with a peak wavelength of 8420 Å (74 Å half-intensity bandwidth) and a half-intensity spatial beamwidth of 38°; when driven with pulses of 50-amps peak current, 150-ns duration, and 5-kHz repetition rate.

Figure 1 is a photograph of a prototype array which includes an optical integrator. The delivered array is identical except for the omission of the integrator. The output end of the fiber bundle is held in a similar brass piece part that has a 23-mil groove.

Figure 1. Injection-Laser Illuminator for 8500 Å

CA32065

SECTION II
LARGE OPTICAL CAVITY LASERS

A. CHARACTERISTICS OF LOC LASERS

Large optical-cavity lasers were first reported by H. Kressel et al.[1] The device consists of a four-layer structure (see Figures 2 and 3): Two confining wide band-gap layers, a thin P-layer with optical gain, and a wave guiding N-layer. The purpose of the N-layer is to distribute the guided optical energy into a larger volume. This reduction of energy density leads to an increase of the threshold value for catastrophic degradation. Single-heterostructure lasers require a 2-microns-wide recombination layer. At energy densities of 1-watt peak power per mil of emitting facet, which corresponds to 2×10^6 W/cm^2, the laser facets are permanently damaged. For LOC lasers, these limits were extended. Values greater than 4 watts per mil for LOC lasers with 6-micron optical cavity have been observed in TI's laboratory.

The drawback of early LOC lasers was their emission beam angle. They exhibited rabbit-ear patterns and until recently had half intensity emission cone angles of 60 to 90° (Figure 4).

The physical mechanism which leads to low threshold currents and high quantum efficiencies is a combination of carrier confinement at the interfaces, with step-like increases of the band gap, and optical confinement because of the reduced optical index in the material with an increased band gap. Because of the difficulties in formulating a mathematical model for the carrier confinement, the LOC structure has so far only been treated in terms of the optical confinement. In a series of publications,[2,3,4,5,6] J. K. Butler applied Maxwell's equations to a multislab structure, assigning different optical indices to the layers. Only the recombination region (thickness d_1 in Figure 3) has optical gain. The computer calculations lead to plots of modal gain vs. cavity dimensions and permit predictions about the order of the mode which will be excited first because of its lowest threshold gain value. Furthermore, the theory permits the calculation of the emission beam pattern. Good agreement between theory and experiments was obtained after reasonable adjustments of the cavity geometric parameters. Despite its complexity, the theory provides guidance for the design of lasers with certain emphasized properties. The theory is, however, not capable of predicting trade-offs between, e.g., beam angle, threshold current, and quantum efficiency. One of the major accomplishments of the theory was the prediction of narrow-beam-angle LOC lasers. Referring to the definition of symbols in Figure 3, the findings of this analysis[2] can be summarized as follows: Narrow beam angles on the order of 20° are exhibited

a.
→ P-TYPE (DIFFUSED GaAs)

→ N-TYPE (GaAs)

DIFFUSED LASER

b.
→ GROWN-P-TYPE GaAlAs

→ OUT DIFFUSED Zn, P-TYPE GaAs

SINGLE HETEROSTRUCTURE "CLOSE CONFINEMENT" LASER

SUBSTRATE

c.
→ GROWN P-TYPE GaAlAs

→ GROWN P-TYPE GaAs

→ GROWN N-TYPE GaAlAs

DOUBLE HETEROSTRUCTURE LASER

→ SUBSTRATE

d.
→ GROWN P-TYPE GaAlAs
→ GROWN OR DIFFUSED P-TYPE GaAs
→ GROWN N-TYPE GaAs
→ GROWN N-TYPE GaAlAs

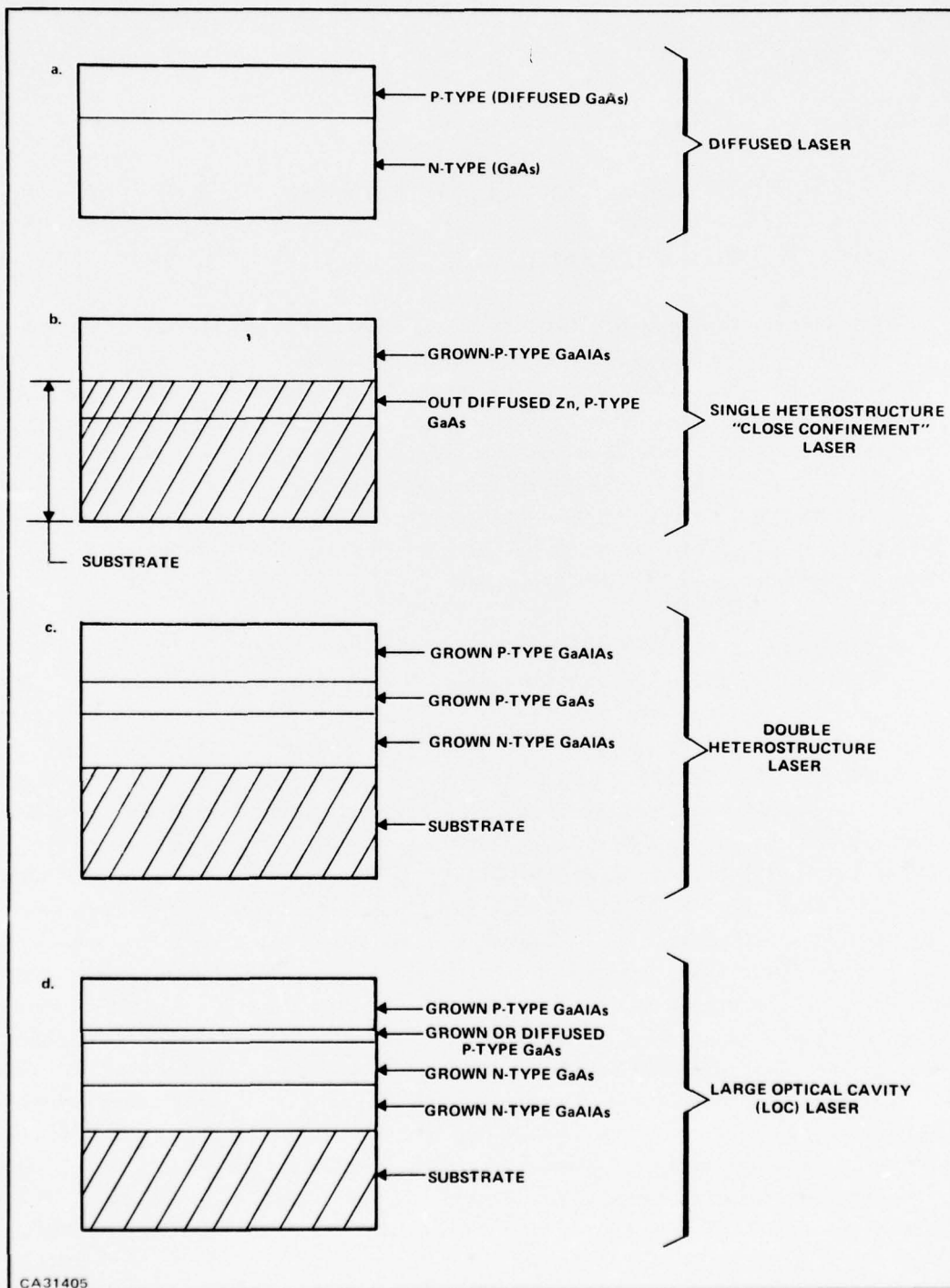LARGE OPTICAL CAVITY (LOC) LASER

→ SUBSTRATE

CA31405

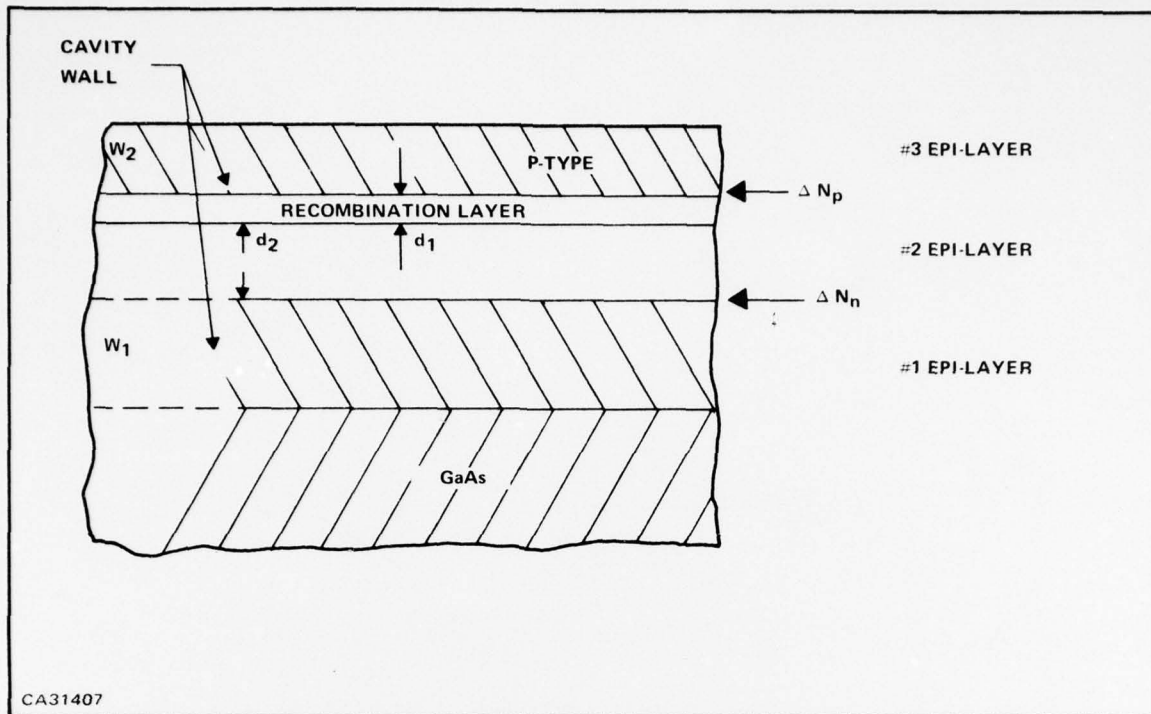Figure 2. Laser Structures (Cross-Sectional Diagrams)

6

Figure 3. Definition of Symbols for the LOC Structure

from structures that have a small index change ΔN_n and an asymmetry factor $f = \Delta N_p/\Delta N_n \geqslant 3$. The structure reported by *Butler and Kressel*[2] had: $\Delta N_n = 0.009$, $f \sim 3$, $d_1 = 1.2$ microns and $d_2 = 5.8$ microns.

To relate the changes of the optical index to the Al concentrations, we show in Figure 5 the index of GaAs vs. the photon energy.[7,8] If one assumes that the addition of small amounts of Al do not change the curve shape, but only cause a parallel shift toward higher energy, one sees that, for a constant photon energy, the optical index is reduced. From the slopes of both plots (taking 10^{20} cm^{-3} for the zinc concentration and $300°$K for the n-type GaAs), one obtains roughly an index change $\Delta N = 0.8/1$ eV, implying a necessary band-gap increase of only 0.0125 eV (corresponding to $\Delta\lambda \sim 100$ Å) at the lower cavity wall to obtain $\Delta N_n \sim 0.01$, as recommended by J. K. Butler and H. Kressel.[2]

By adjustment of the aluminum concentrations in layers #1, #2, and #3, the half-intensity emission cone angles of the LOC lasers grown for the array of this report were reduced to approximately 45°. While smaller emission cone angles can be achieved, there is a trade-off in output power. Figure 6 is a beam intensity versus angle recording for LOC slice No. 14090-20, which was used for the array.
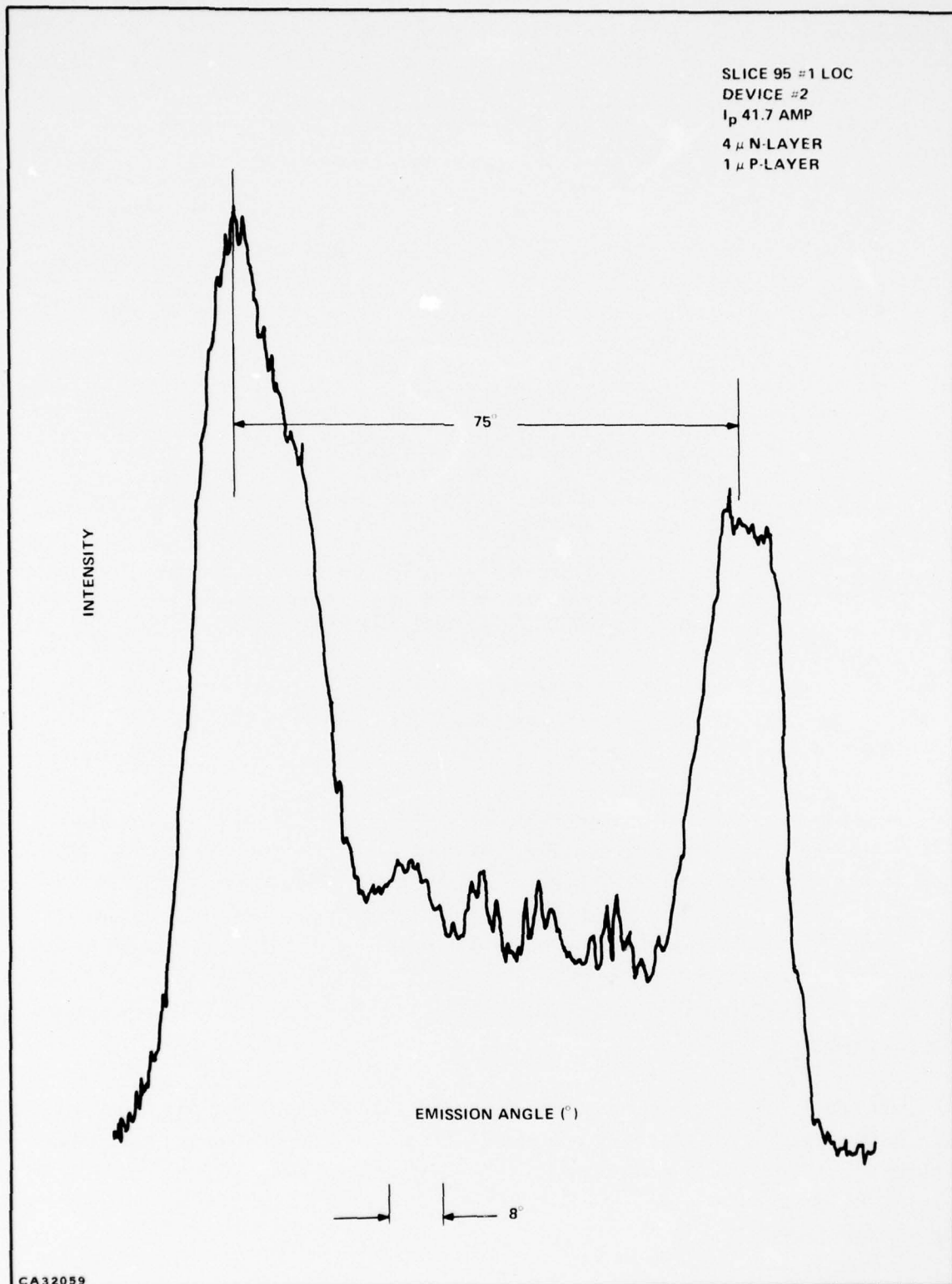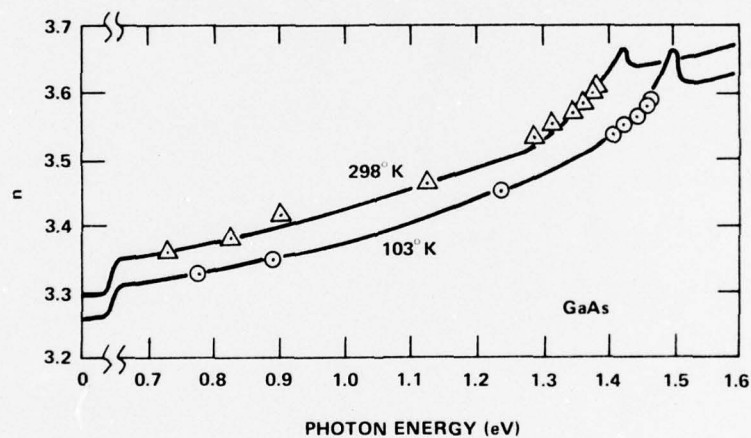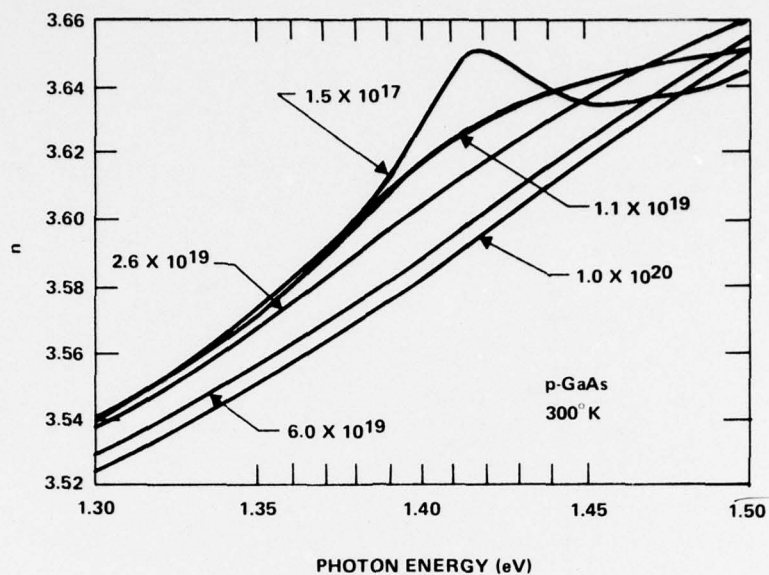
Figure 4. Beam Intensity versus Angle Normal to Junction

Top graph (p-GaAs, 300°K): n versus PHOTON ENERGY (eV), with curves labeled 1.5 × 10^17, 1.1 × 10^19, 1.0 × 10^20, 2.6 × 10^19, 6.0 × 10^19.

1.5 X 10^{17}

1.1 X 10^{19}

2.6 X 10^{19}

1.0 X 10^{20}

6.0 X 10^{19}

p-GaAs
300° K

PHOTON ENERGY (eV)

Middle graph (GaAs): n versus PHOTON ENERGY (eV), curves for 298° K and 103° K.

298° K

103° K

GaAs

PHOTON ENERGY (eV)

$$\lambda = \frac{1.24}{eV}$$

	$\lambda = \dfrac{1.24}{eV}$	$\dfrac{\Delta\lambda \ (\text{Å})}{0.1 \ \Delta eV}$	$\dfrac{\Delta n}{\Delta 100 \ \text{Å}}$
	1.6 eV	7750 Å	520	0.015
	1.5 eV	8270 Å	580	0.014
GaAs →	1.4 eV	8850 Å	700	0.011
1.38 eV	1.3 eV	9550 Å	750	0.011
	1.2 eV	10300 Å		

$$\frac{\Delta n}{\Delta eV} = \frac{0.8}{1 \ eV} = \frac{0.08}{0.1 \ eV}$$

APPROXIMATELY 100 Å ≏ Δn ~ 0.01

BLACKNALL (880 GROWTH) 50 Å PER 1 mg Al

CA31408

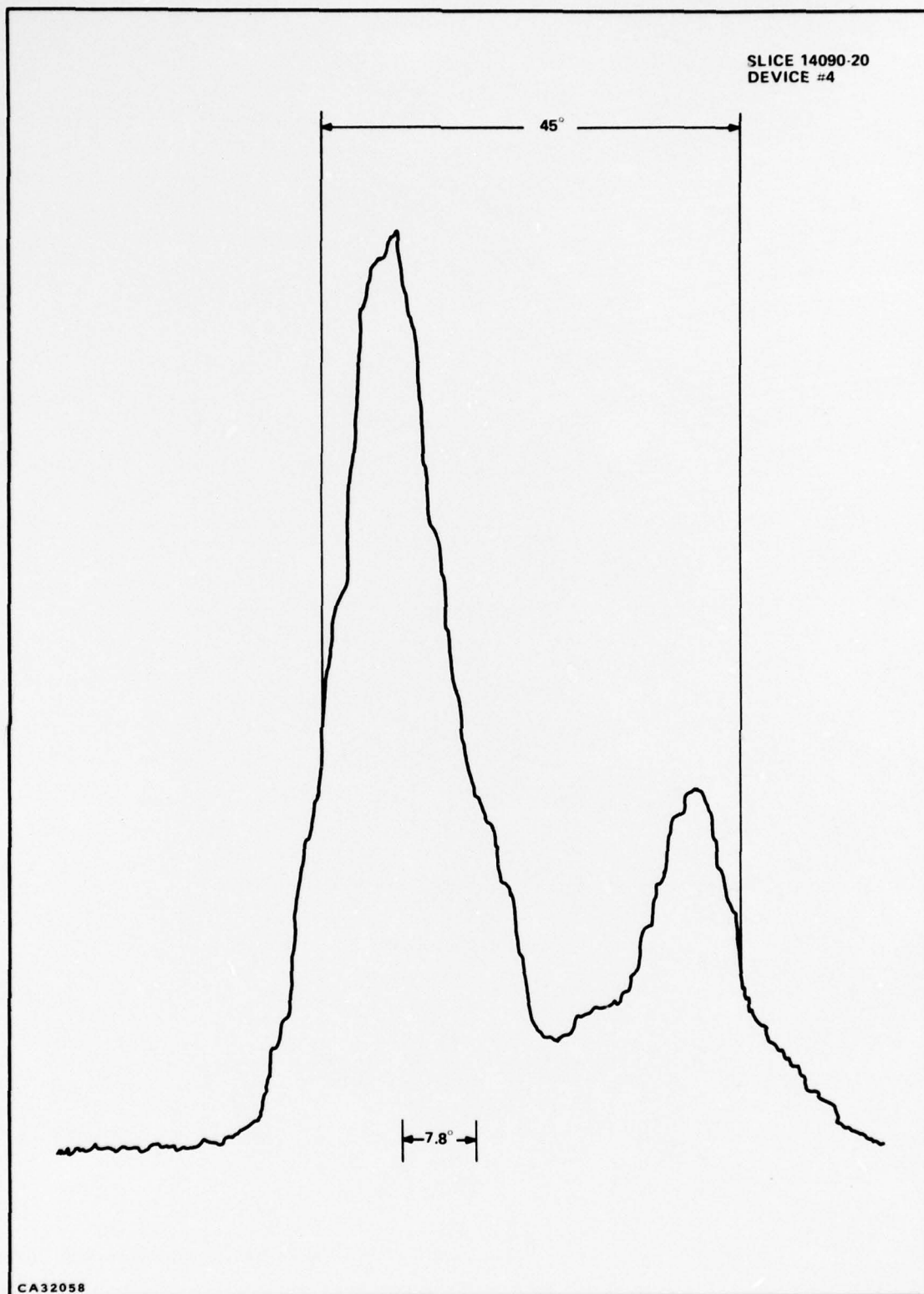Figure 5. GaAs Refractive Indices versus Photon Energy

9

Figure 6. Emission Intensity versus Beam Angle

B.   LIQUID EPITAXIAL GROWTH

The heterostructure lasers are grown by a liquid-phase epitaxial process in a multibin sliding-boat system. A graphite boat for a two-layer structure is shown in Figure 7. The boat is heated, in a quartz tube filled with Pd-diffused hydrogen, by a three-zone diffusion furnace. The profile is flat, over the length of the boat, within $1.25°C$. During growth, the furnace is cooled by a synchronous motor turning the temperature control.

The thermocouples are of platimun/platinel II, which is as stable as Pt/PtRh, but generates a thermovoltage similar to chromel/alumel. A two-hour hydrogen flush was used to sweep the air from the tube.

Ga and GaAs are homogenized at high temperature (e.g., $950°C$) and the other dopants (Al, Zn, Te) are added to the melts prior to the actual run. For the run of LOC slice No. 14090-20 the furnace with the loaded graphite boat was heated to $900.0°C$, then cooled at the rate of $1°C$/minute. The first epitaxial layer was grown from $890-887°C$, the second layer from $887-884°C$, and the third layer from $884-876°C$.

For the run under discussion, melts oversaturated with GaAs were employed, i.e., 2.5 g GaAs/15 g Ga at growth temperatures between $890°C$ and $850°C$.

The melt composition and performance of narrow-beam-angle LOC slice No. 14090-20 are shown in Table I. The half-intensity beam width is $\alpha_{1/2}$. The thickness of the grown second layer is

Table I. Composition and Performance of LOC Slice No. 14090-20

Melt Compositions			Ga in Melt = 15 gm				
GaAs (g)	Al-Concentration 3/2/1 Layer (mg)	Zinc, Te 2 Layer (mg)	Geometry d_1, d_2 (μ)	$\alpha_{1/2}$ (degree)	I_{th} (kA)	λ (A)	η_{sl} (WA^{-1})
2.5	15/4.55/5.75	200, 2	1, 5.5	45	25	8420	0.5

$d_1 + d_2$. During the growth of the third layer, zinc diffuses into the second layer thus forming the recombination layer (d_1).

C.   CHIP FABRICATION

The fabrication of laser devices is a straightforward process. The [100] oriented slice with the deposited epitaxial structure is lapped from the N-side to approximately 4 mils in thickness; both sides are metallized, using a plated Au layer, and are then alloyed. Laser facets are formed by
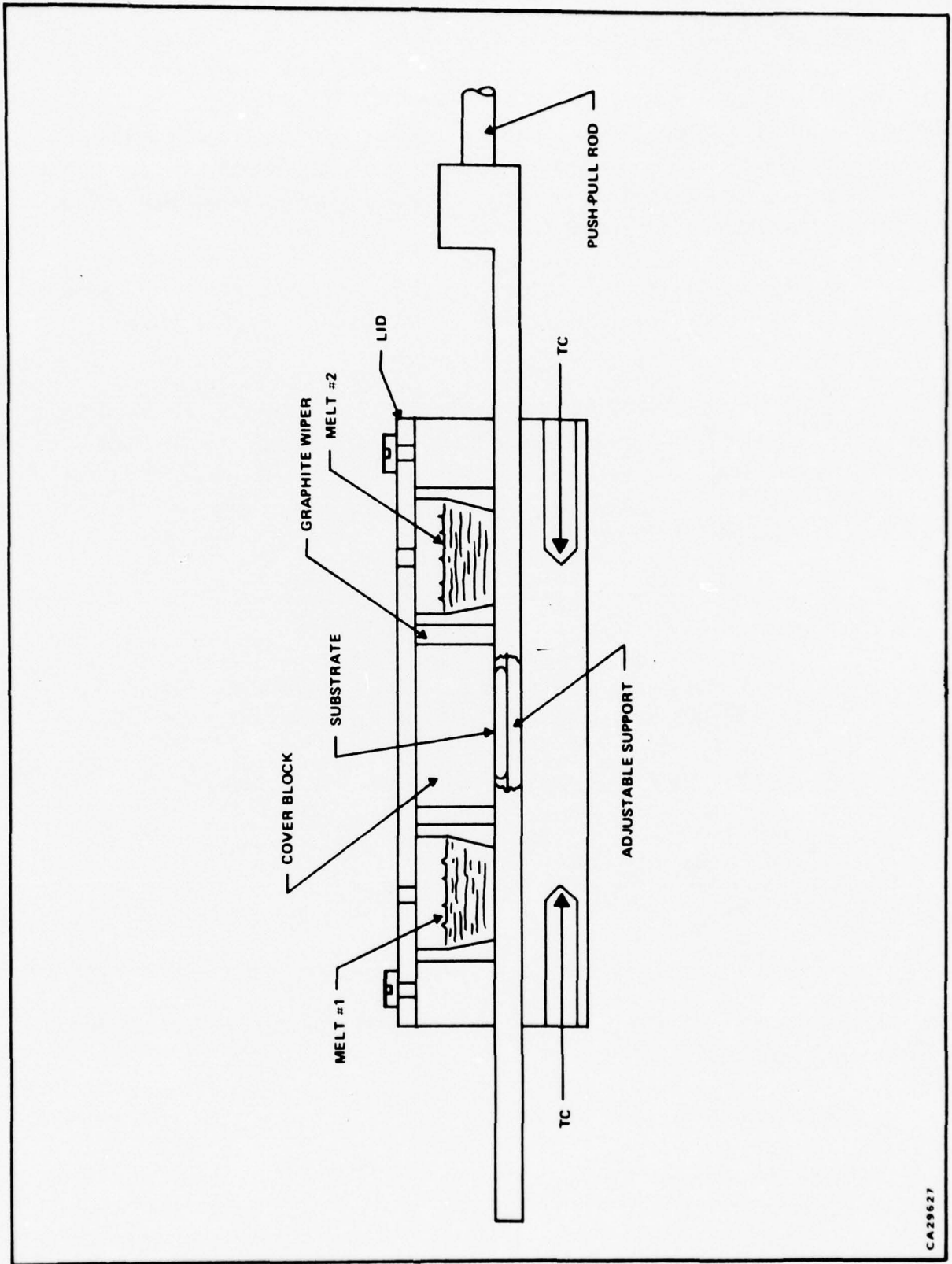
Figure 7. Sliding-Boat Solution-Growth System

CA29627

12

cleaving along the [100] plane. Lateral lasing modes are suppressed by roughening the sides before soldering the chip to a header. To apply a mirror coating, a sandwich of SiO-Cr-Au-Cr-SiO is evaporated onto the cleaved facet opposite the emission facet.

SECTION III
FABRICATION TECHNIQUES

A.   FIBER-COUPLED-DIODE ASSEMBLY

Individual fiber-optic-coupled laser-diode assemblies are constructed as shown in Figure 8. This assembly is fabricated by first soldering (with 60/40 solder) the laser diode chip (P-side down) to the copper piece part. The chip is 10 mils by 10 mils in area. The N-contact is then covered with KMER and a mirror coating is evaporated on the back side of the chip. The mirror coating is a sandwich of SiO-Cr-Au-Cr-SiO. The KMER is then removed and the H-film strip is soldered to the copper piece part using 60/40 solder. The copper tab on the H-film which extends beyond the insulation, is then soldered to the laser chip N-contact using 117°C solder.

The clearance groove in the copper piece part allows the fiber-optic ribbon to be aligned directly against the front of the laser chip with no interference from excess solder.
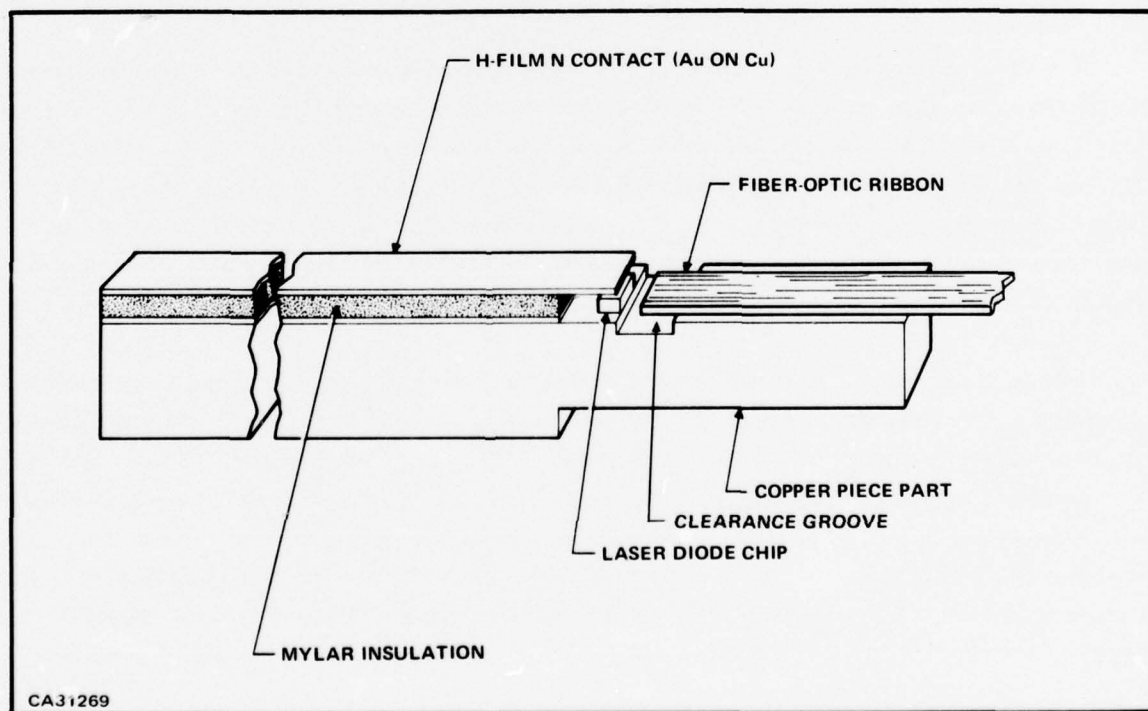

Figure 8. Fiber-Optic-Coupled Laser Diode Assembly

The fiber-optic ribbon (see the Appendix) is attached in a special jig which allows the diode to be electrically pulsed while the fiber is aligned in three dimensions for optimum light transmission. Before alignment, a drop of clear, epoxy cement couples the ribbon optically to the laser facet. When the fiber ribbon has been positioned for maximum light output, a drop of Vigor cement (alpha cyanoacrylate) is applied between the copper piece part and the glass ribbon. This bond hardens in about two minutes. An additional quantity of clear epoxy is added to increase mechanical strength, and the completed assembly is set aside to cure. Figure 9 shows four views of one such laser-diode assembly. The discoloration of the copper piece part is due to the mirroring process.

B.   MODULE ASSEMBLY

The array consists of two modules of 9 diodes each. Each module is constructed as shown in Figure 10.

To assemble the module, nine laser-diode assemblies were stacked as shown in Figure 10, but on a flat table surface. The stack of diodes was pressed together between two pieces of brass weighing about one pound each. Epoxy was then spread over the sides of the diode assemblies and allowed to cure in place. The cemented-together nine-diode group was then bonded to the anodized-aluminum support bracket by thermal conductive epoxy (Emerson and Cuming Stycast 285OFT).

The very critical bundling of the nine loose optical-fiber-ribbon output ends was accomplished in the following manner: The ends of the nine ribbons were constrained to lie in one plane by supporting the ends of a glass slide (see Figure 11). Two brass blocks were used to push the ribbons together and to hold them in approximate alignment as needed for assembly into the array. A third brass block with a section of glass slide attached was used to push against the ends of the ribbons so that the end of the bundle was flat. With all three dimensions thus fixed, a drop of cement was applied at position "x" (Figure 11, top view) and allowed to cure.

Two modules with ribbons pre-bundled as described were secured by a screw to an anodized aluminum frame as shown in Figure 12. The two bundles of ribbons were fitted into a 23-mil wide by 20-mil deep groove cut in a brass block. Originally, a 20-mil by 20-mil by 400-mil flint-glass optical integrator was placed in the same groove, and coupled to the output end of the fiber bundle with clear epoxy. But it was found that the emission pattern obtained when the optical integrator was used was unacceptable, so the integrator was omitted. Section V contains more details on the integrator emission. The delivered array has the end of the fiber bundle extending about 1/16 inch beyond the end of the groove in the brass block. The emission aperture is ~ 15 mils by 20 mils.
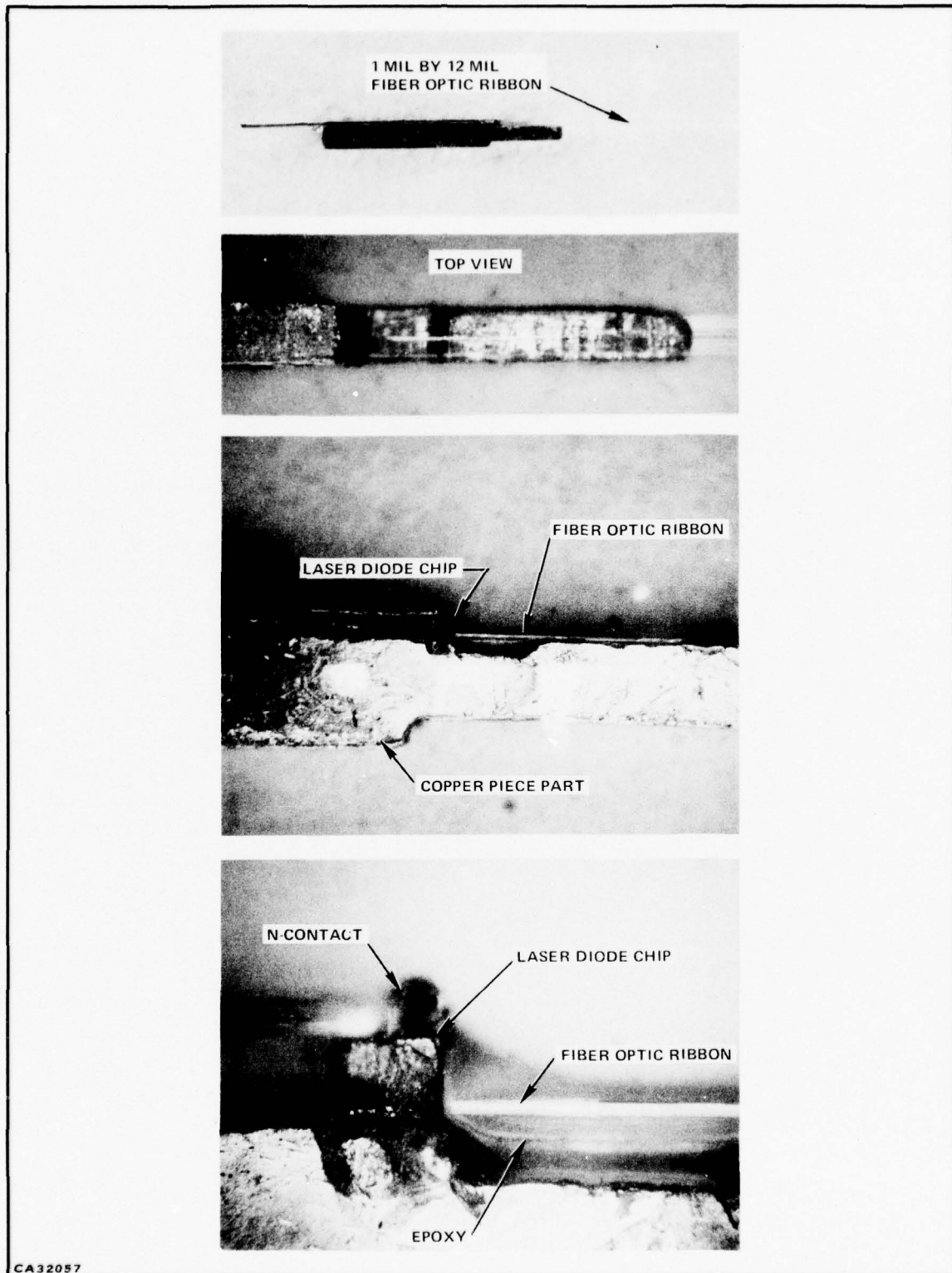
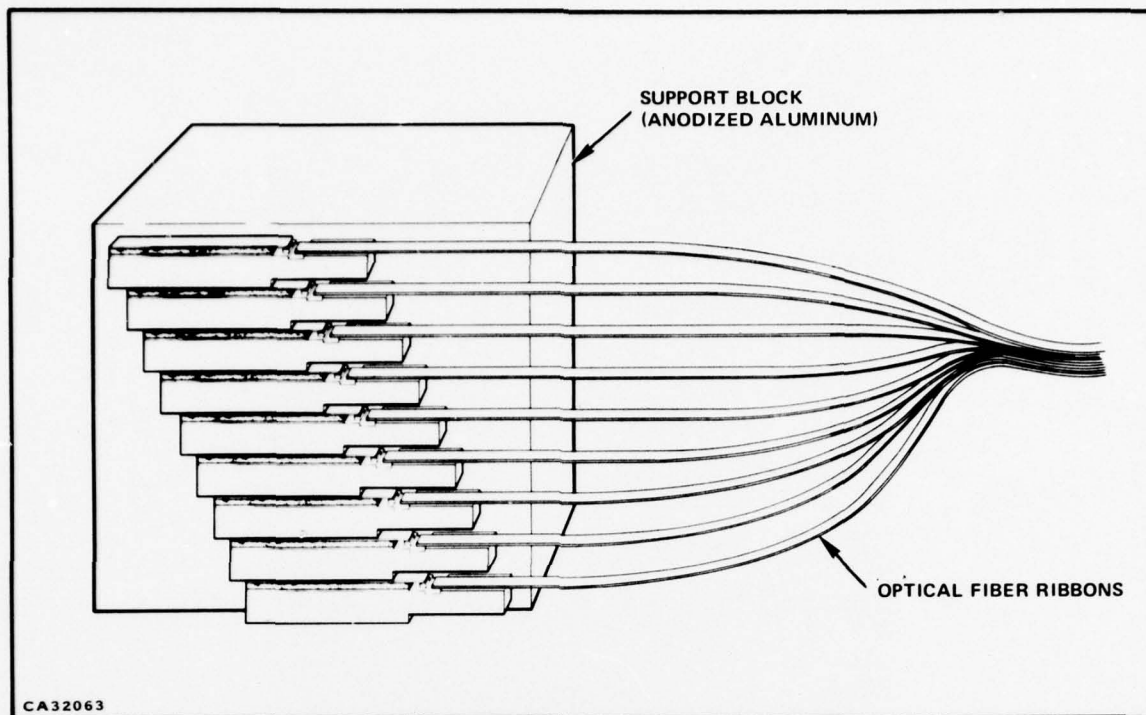Figure 9. Fiber-Optic-Coupled Laser Diode Assembly

17

Figure 10. Module Construction

TOP VIEW

GLASS SLIDE SECTION

NINE-DIODE MODULE
ON SUPPORT BLOCK

BRASS
POSITIONING
BLOCK

X

BRASS POSITIONING
BLOCKS

OPTICAL FIBER RIBBONS

GLASS SLIDE

SIDE VIEW

GLASS SLIDE

DIODE MODULE

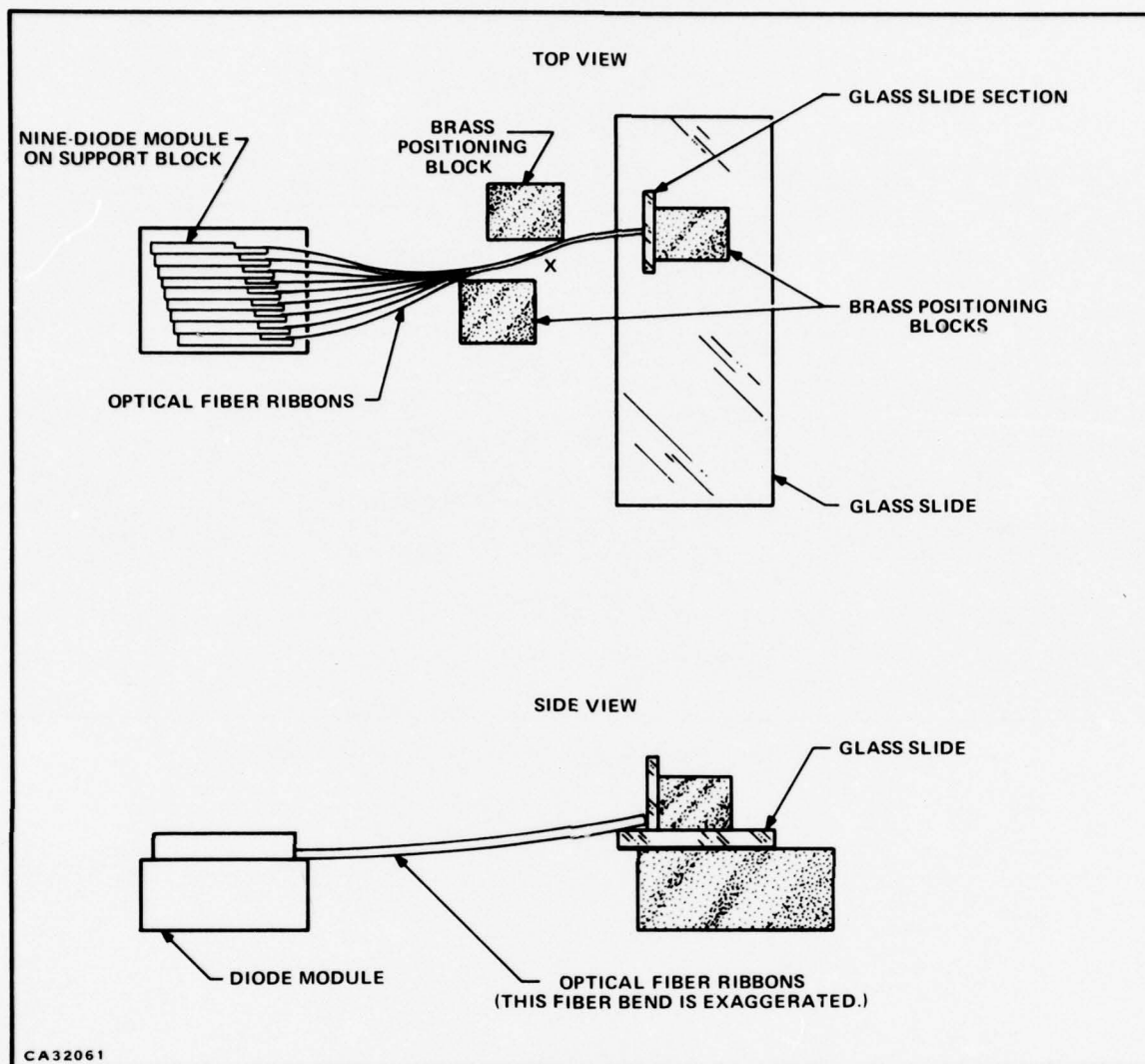OPTICAL FIBER RIBBONS
(THIS FIBER BEND IS EXAGGERATED.)

CA32061

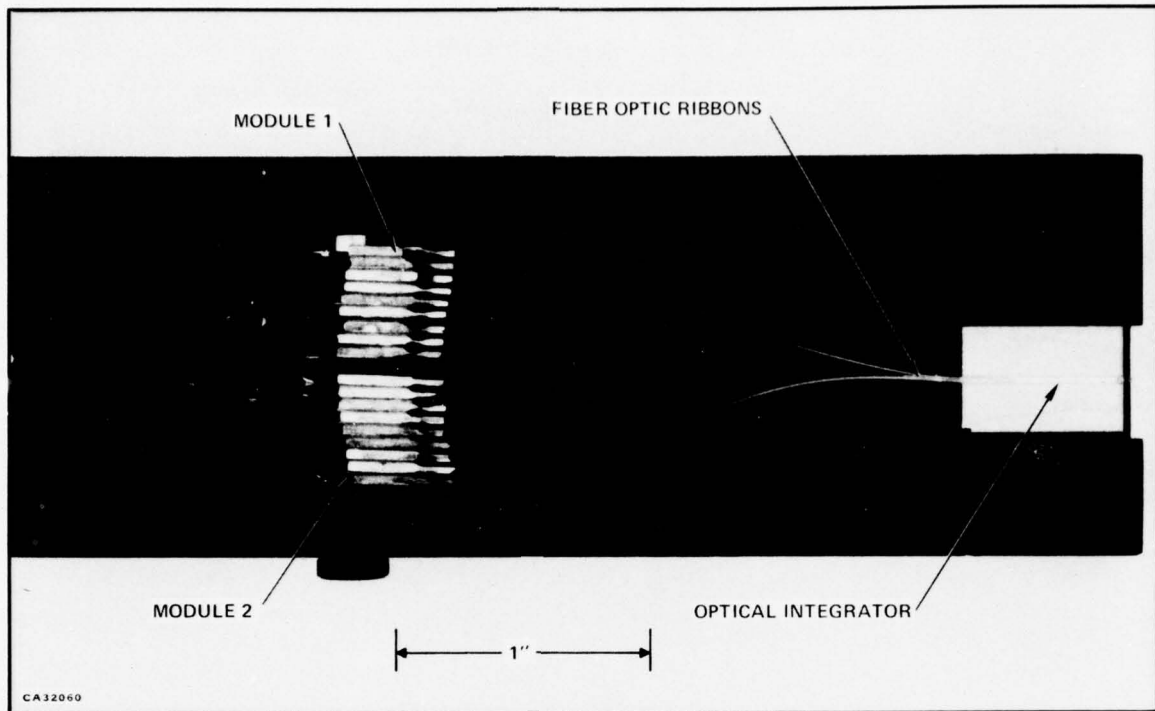Figure 11. Optical Fiber Ribbon Bundling

Figure 12. Injection-Laser Illuminator Array for 8500 Å Emission

SECTION IV
ELECTRO-OPTIC EVALUATION

A. EQUIPMENT

The array was electrically driven by a Velonex Model 380 High Power Pulser. The peak current was monitored by the ferrite-toroid transformer circuit of Figure 13. Using a precision, low-inductance 1-ohm resistor for current sampling, the transformer has been calibrated at 60 mV/amp.

All waveforms are displayed on a Tektronix Type 546 oscilloscope. Voltage readings are made using the Tektronix 10X probe.

All optical power measurements were made with an ITT F4000 (S-1) photodiode, calibrated at 0.95 mA/watt in the 8400 to 8500 Å spectral region.
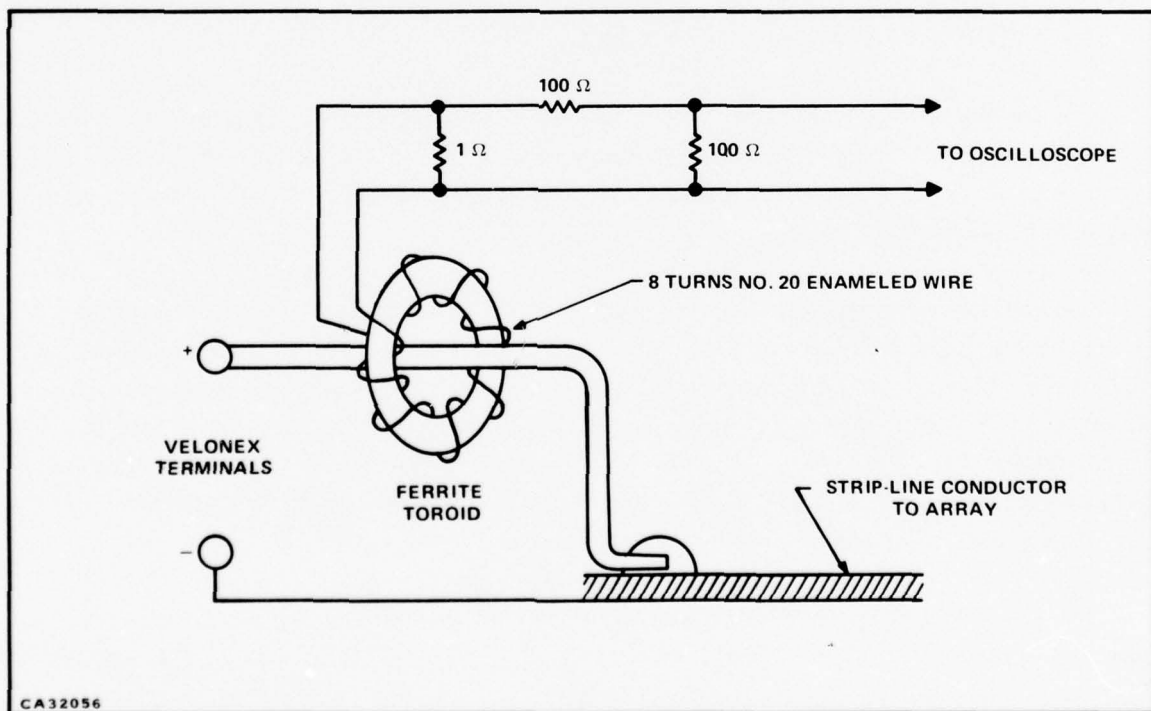

Figure 13. Current Transformer

21

Wavelength was measured by a Jarrell-Ash Model 82-020 grating spectrometer with thermoelectrically cooled Type-7102 photomultiplier.

B.   PERFORMANCE DATA

Because the Velonex pulser was unable to drive the entire array, all measurements were made on one module at a time. The modules are called "1" and "2" as indicated in Figure 12.

For the intensity versus wavelength plot of Figure 14, each module was driven with 150-ns wide pulses, with a rise time of < 10 ns and a fall time of < 20 ns, peak current of 50 amp, and a pulse repetition rate of 500 Hz. The center wavelength is 8420 Å at half-intensity.

Peak power emitted, P_o, was measured as a function of peak current. The pulse width was 150 ns and the frequency 100 Hz. The result is presented in Figure 15. At 50-amps peak drive current, module No. 1 emitted 57 watts peak, and module No. 2 emitted 48 watts.

For power measurements, the width of the electrical pulse is very important. The beginning of the optical pulse lags the electrical pulse by about 40 ns, and the optical pulse has a long rise time. For a pulsewidth less than ~ 125 ns, the optical output does not reach its peak value. For an electrical pulsewidth greater than ~ 200 ns, the peak optical power will decrease due to heating during the pulse. This is illustrated by the idealized waveforms of Figure 16. For the delivered array, the optimum electrical pulse width is approximately 150 ns.

The outputs of the two modules were summed arithmetically to yield the power versus current plot of Figure 17. At 100 Hz, the sum is 105 watts at 50 amps and 131 watts at 67 amps. AT 5 kHz frequency, the total power is 84 watts at 50 amps, measured in less than 5 seconds, so that long-term heating was not involved.

Because the injection lasers used in this array are of the large-optical-cavity structure, the emission-beam angle and spatial intensity pattern of the output beam are of particular importance. The far-field intensity patterns for each module separately, and both modules driven together, at 45 amps, 1 kHz, 150-ns pulsewidth, were investigated by projecting the beam on a sheet of graph paper attached to a glass plate, and scanning the intensity pattern with a 1-mm diameter silicon photovoltaic detector. The beam patterns are similar in gross features to the pattern of a single LOC-laser diode (as in Figure 6), but somewhat smoother.

The plots of Figure 18 show the spatial distribution of the intensity maxima (lobes of the LOC emission), denoted by "x", the relative minima points of intensity equal to one-half the maximum, denoted by "●". In each case, the highest intensity point in the field pattern was located and
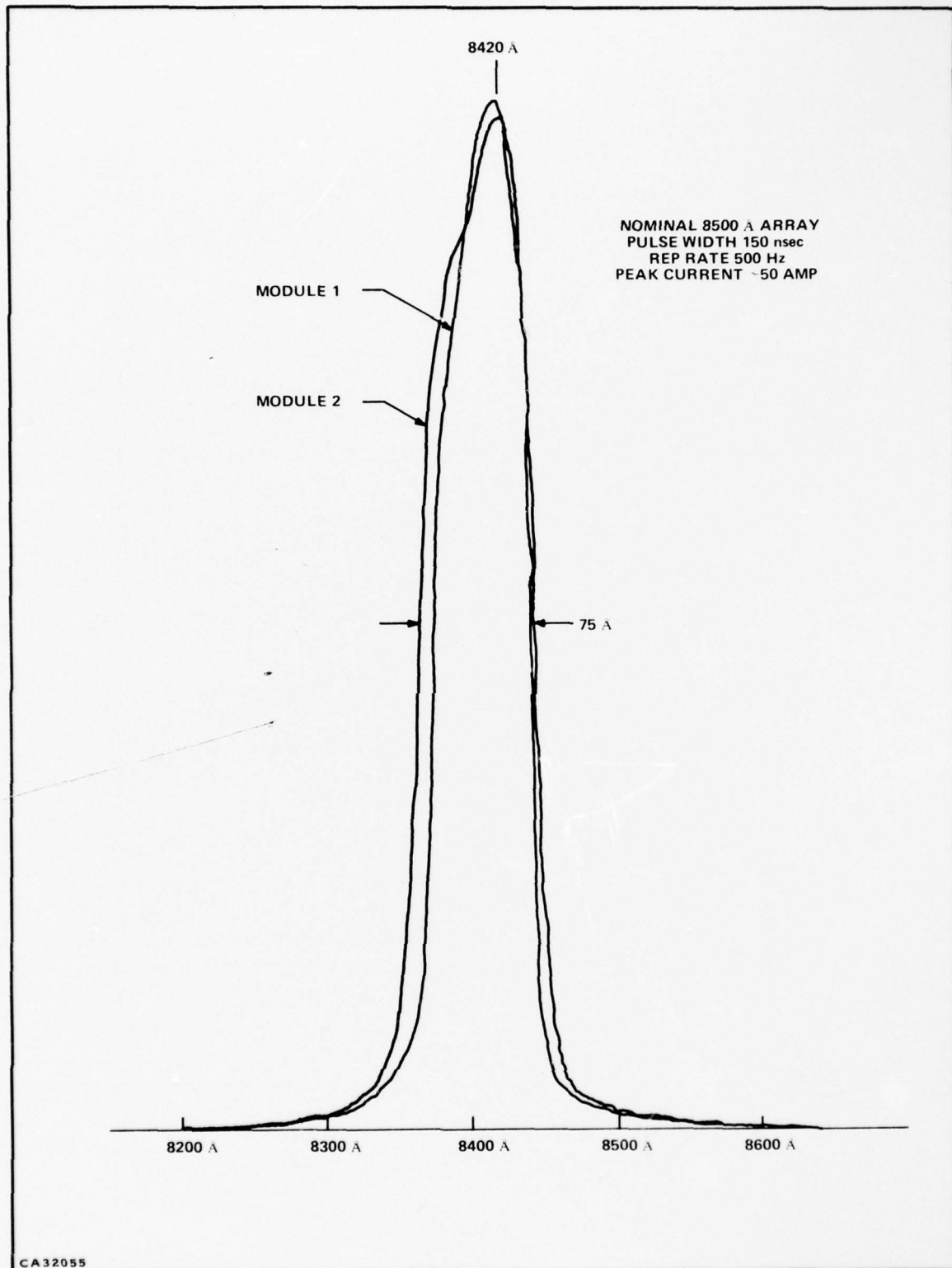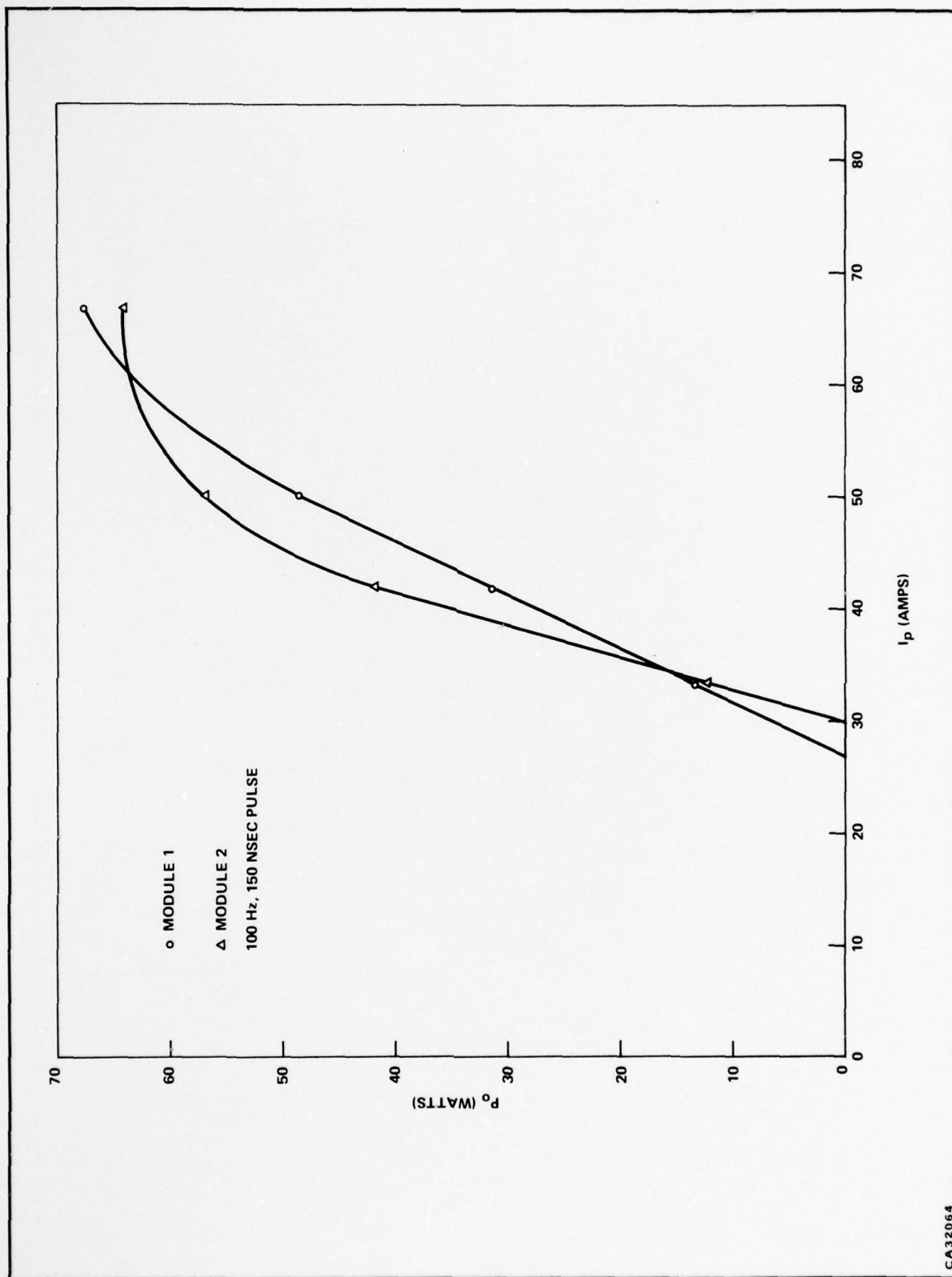
Figure 14. Array Emission Spectrum

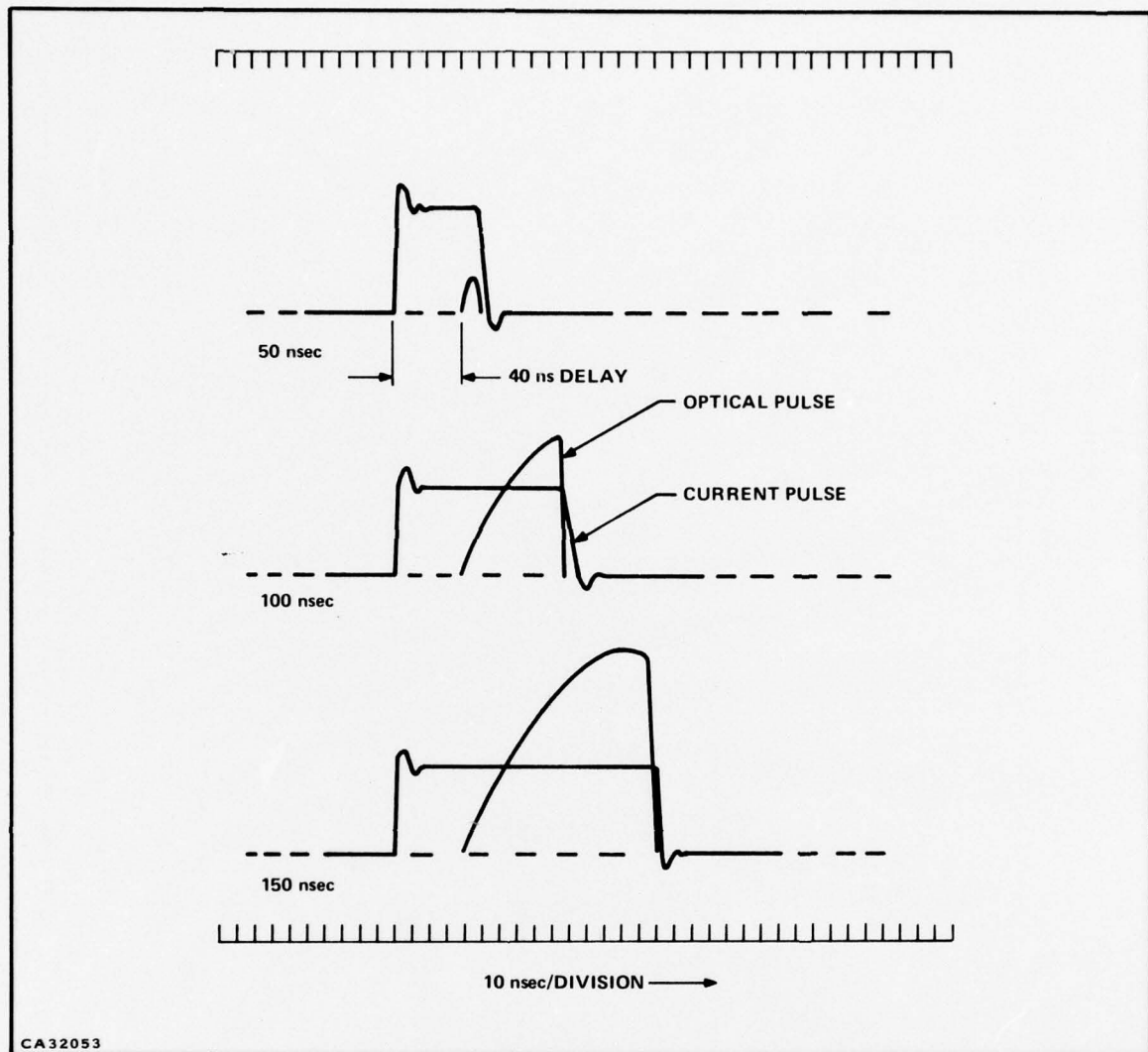Figure 15. Emitted Peak Power versus Peak Current

24

Figure 16. Optical Pulse Peak Amplitude Dependence on Electrical Pulse Width

normalized to an amplifier reading of 1. All other points were then referenced to that peak, so that in the case of Module No. 1, the other lobe has an intensity of .9, and the intensity of the central relative minimum is 0.75. The beam angle at half-maximum intensity in the plane of greatest spread (perpendicular to the plane of the P-N junctions) was calculated from the geometry shown in the inset of Figure 18.

The original array design required a 20-mil by 20-mil by 400-mil glass cell to be fixed to the output end of the optical fiber to provide mixing or integration of the multiple emission beams, so that the far-field pattern would be more uniform. Such an integrator was optically (epoxy) coupled
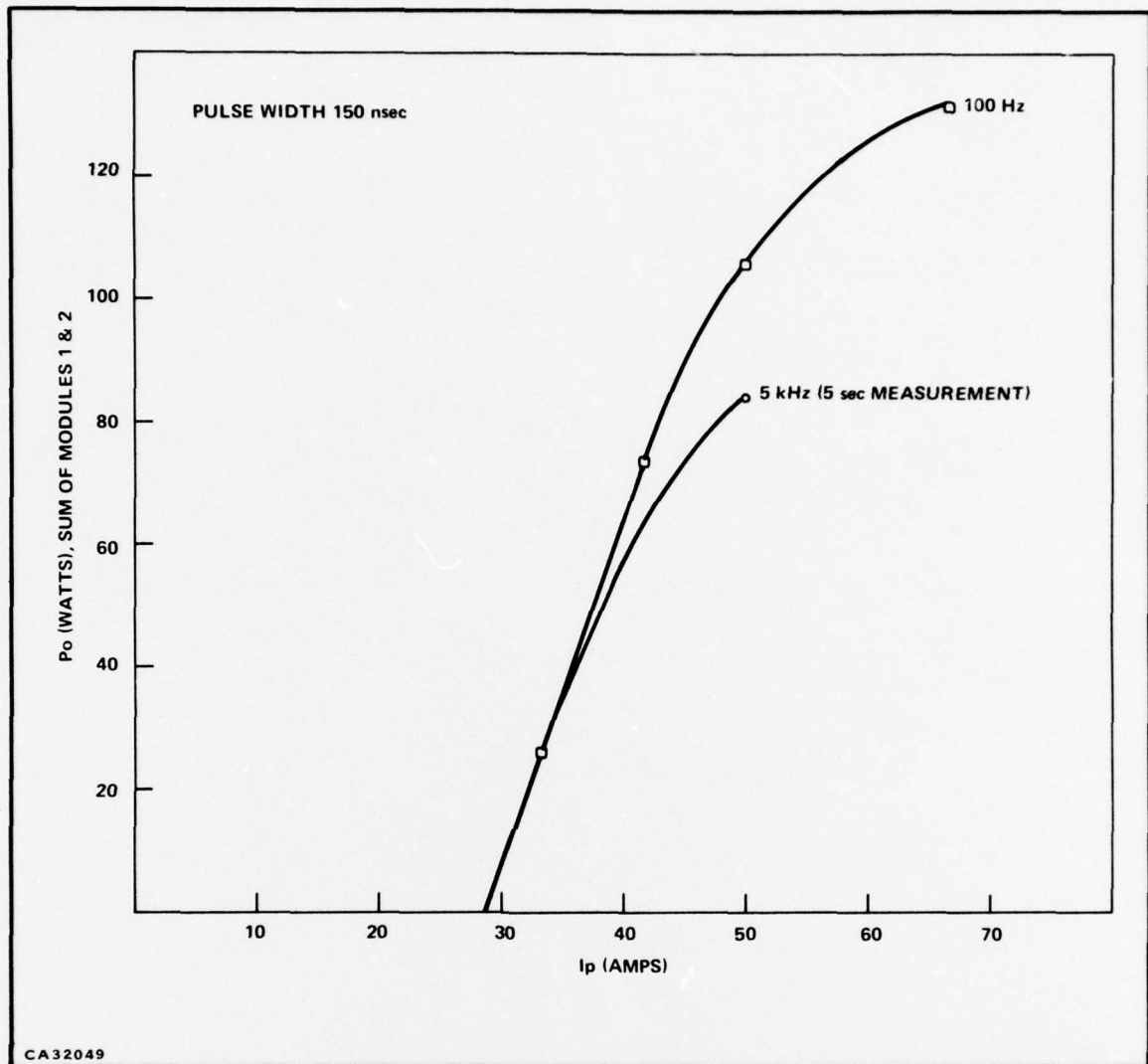
Figure 17. Sum of Peak Powers Emitted by Modules 1 and 2

to the prototype array (Figure 12), but the intensity pattern, rather than being smoothed, became, on a screen perpendicular to the beam axis, a two-dimensional array of roughly rectangular bright spots with a "line" structure and an overall intensity diminishing with the radius. Figure 19 is an approximate drawing of the observed intensity distribution on a white card held about two inches from the emission aperture.

The same pattern was observed whether the total array was lasing or spontaneously emitting, and when one diode only was either lasing or spontaneously emitting.
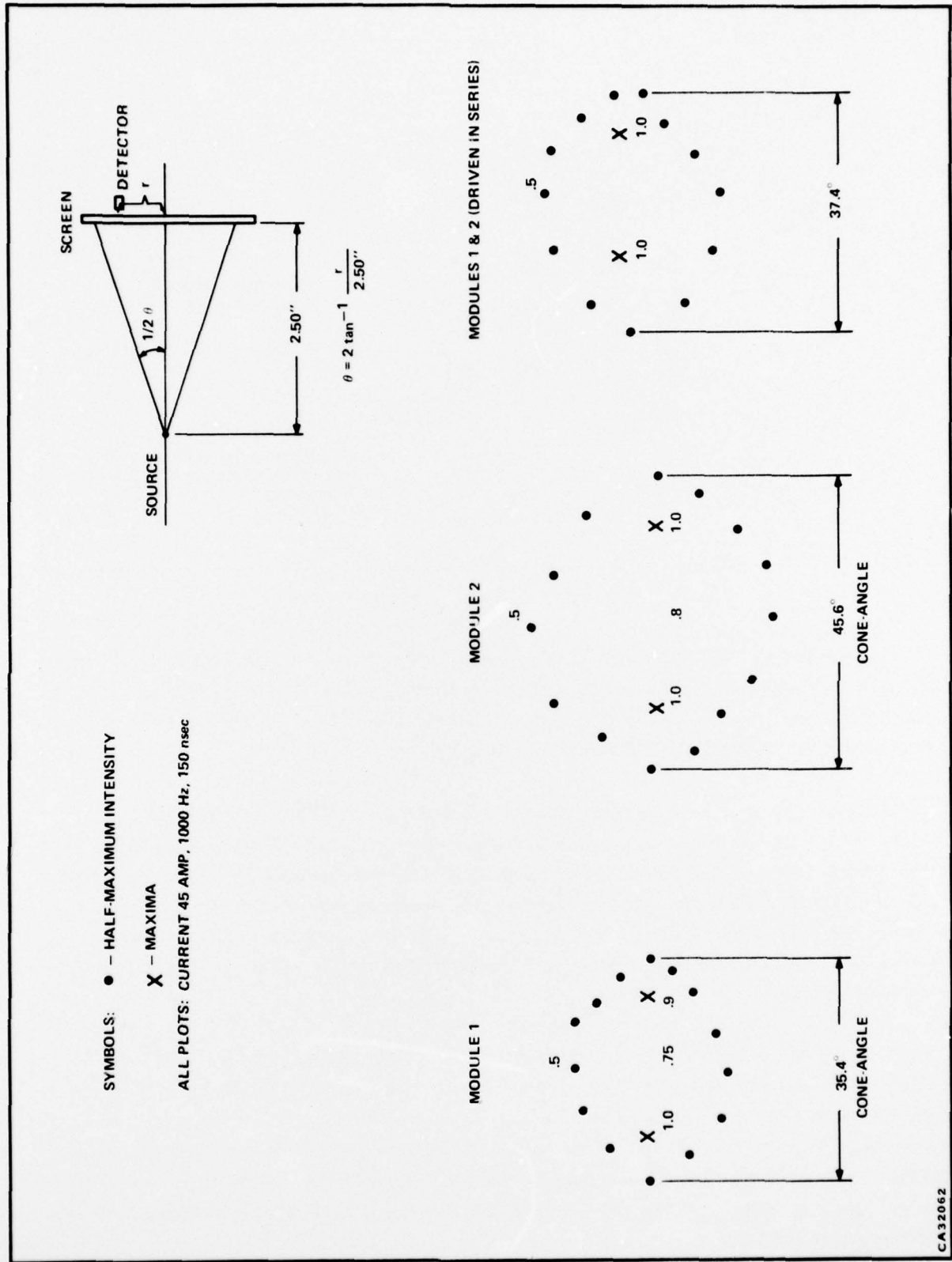
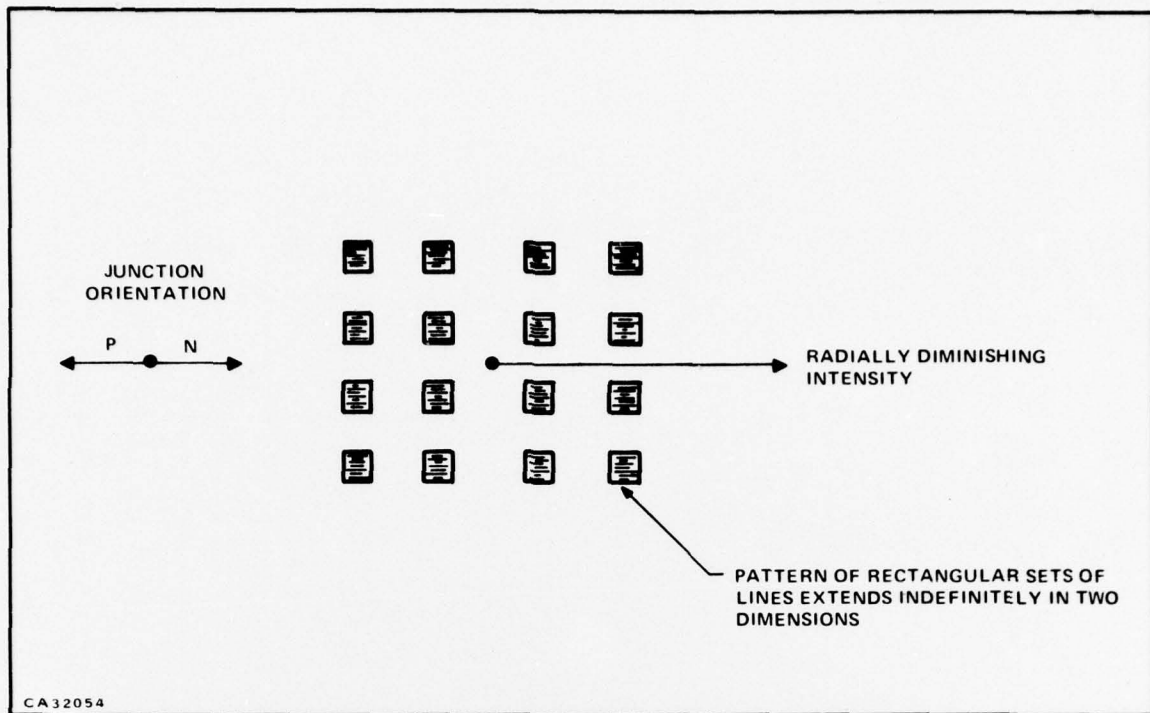Figure 18. Far-Field Beam Intensity Patterns

Figure 19. "Integrator" Emission Intensity Pattern

The effect is apparently due only to the geometry and reflectivity of the integrator and optical fiber system; however, *the phenomenon is not understood in detail.* Due to this phenomenon, the optical integrator was omitted from the delivered array. The integrator reduced the total peak power available from the optical fiber bundle by about 10%.

The peak power emitted by each module was measured at 100 Hz, 1 kHz, and 5 kHz. The readings were taken in less than ten seconds each, so that heating was limited. At 50-amps peak drive current, the sum of the peak power emitted from the two modules is 106 watts at 100 Hz, while at 5 kHz the sum is 84 watts. The power versus frequency plot, Figure 20, shows an increase in power for Module No. 1 when the frequency increases from 100 Hz to 1 kHz. Whether or not this is a measurement error is not known, but the same phenomenon was observed in another laser array measurement.[9]

With a peak current of 50 amps, a pulsewidth of 150 ns, and the frequency at 5 kHz, each module was operated separately for two minutes, and the peak power was measured as a function of time (Figure 21). At the end of two minutes, the power was very nearly stable, with the power falling from 57 watts to 39 watts for Module No. 1, and from 28.5 watts to 23 watts for Module No. 2. At the end of the two minutes, the drive current was removed and the modules were allowed to cool for 30 seconds. The output of Module No. 1 increased to 47.5 watts and that of Module No. 2 increased to 25 watts.
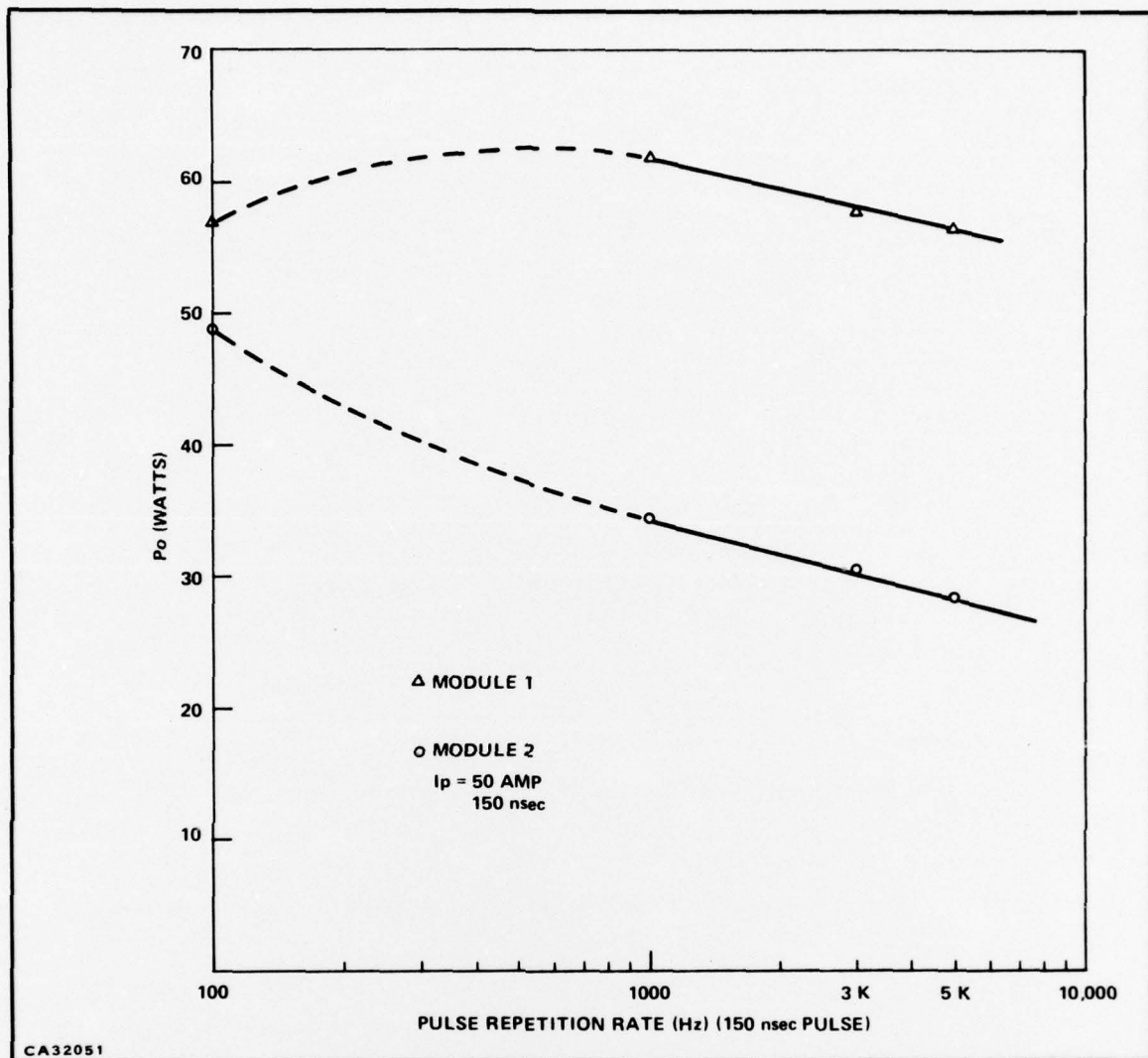
28

Figure 20. Power versus Frequency

The frequency response of the array was adversely affected by the rather high series resistance. As shown in Figure 22, the series resistance of Module No. 1 is 1.1 ohms, or 0.12 ohm/diode, and for Module No. 2 the resistance is 1.6 ohms, or 0.178 ohm/diode. The reason for this is that no P-type GaAs layer was grown on the material from which the diodes were fabricated. This extra layer has been found necessary to facilitate ohmic contacts to GaAlAs. Due to the high series resistance, the power efficiency (based on the formula $\eta_p = P_o/I_p V_p$) for the total array at 50-amps drive current at 100 Hz is 1.5%.

29
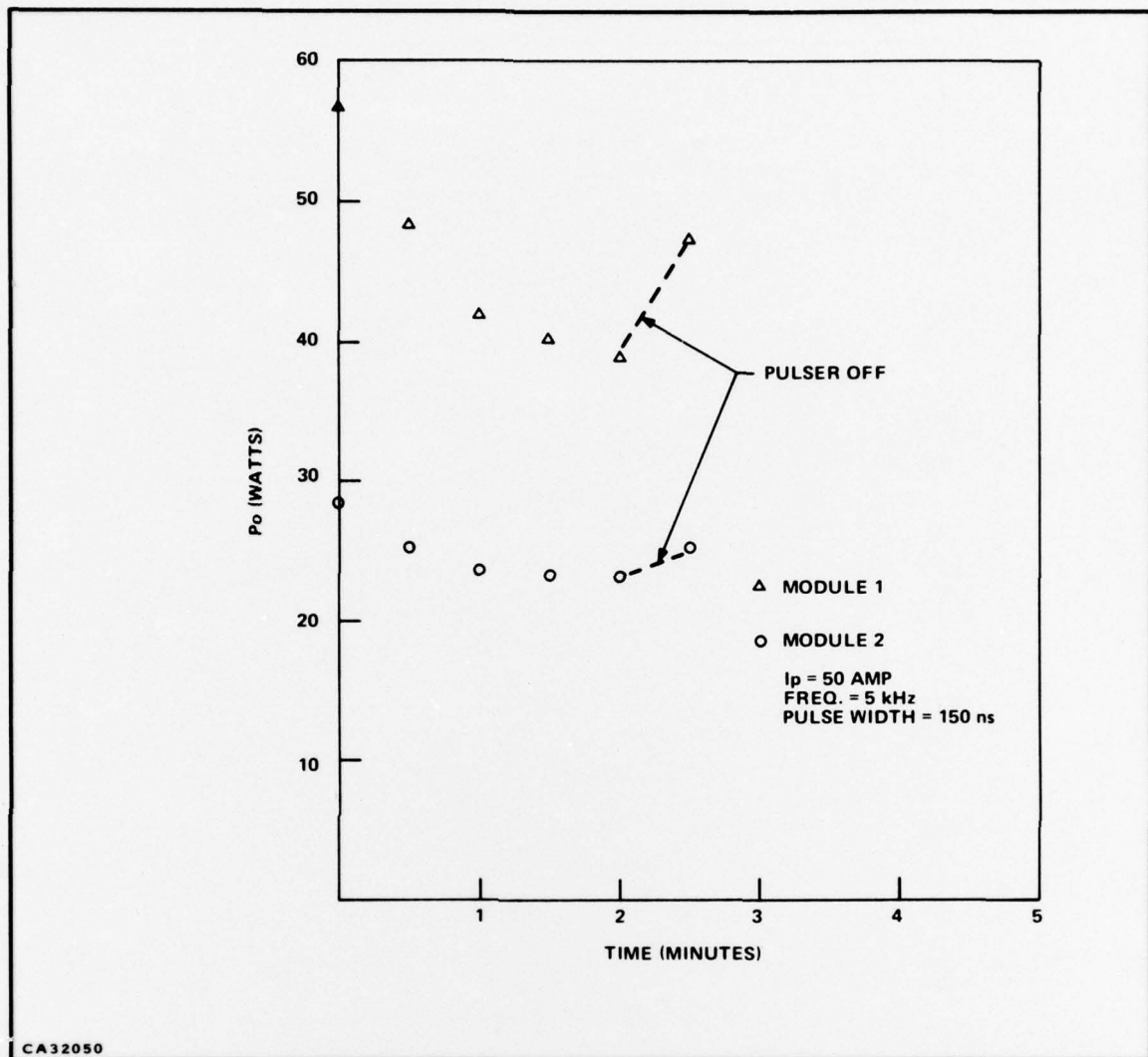
Figure 21. Power versus Operating Time

A summary of measured performance is shown below:

Spectral peak wavelength	8420 Å
Spectral half-width	75 Å
Peak power at 100 Hz, 150 ns, 67 amp	132 W
Peak power at 100 Hz, 150 ns, 50 amp	106 W
Peak power at 5 kHz, 150 ns, 50 amp	84 W
(short-term operation)	
Peak power at 5 kHz, 150 ns, 50 amp	62 W
(after 2-min operation)	

30
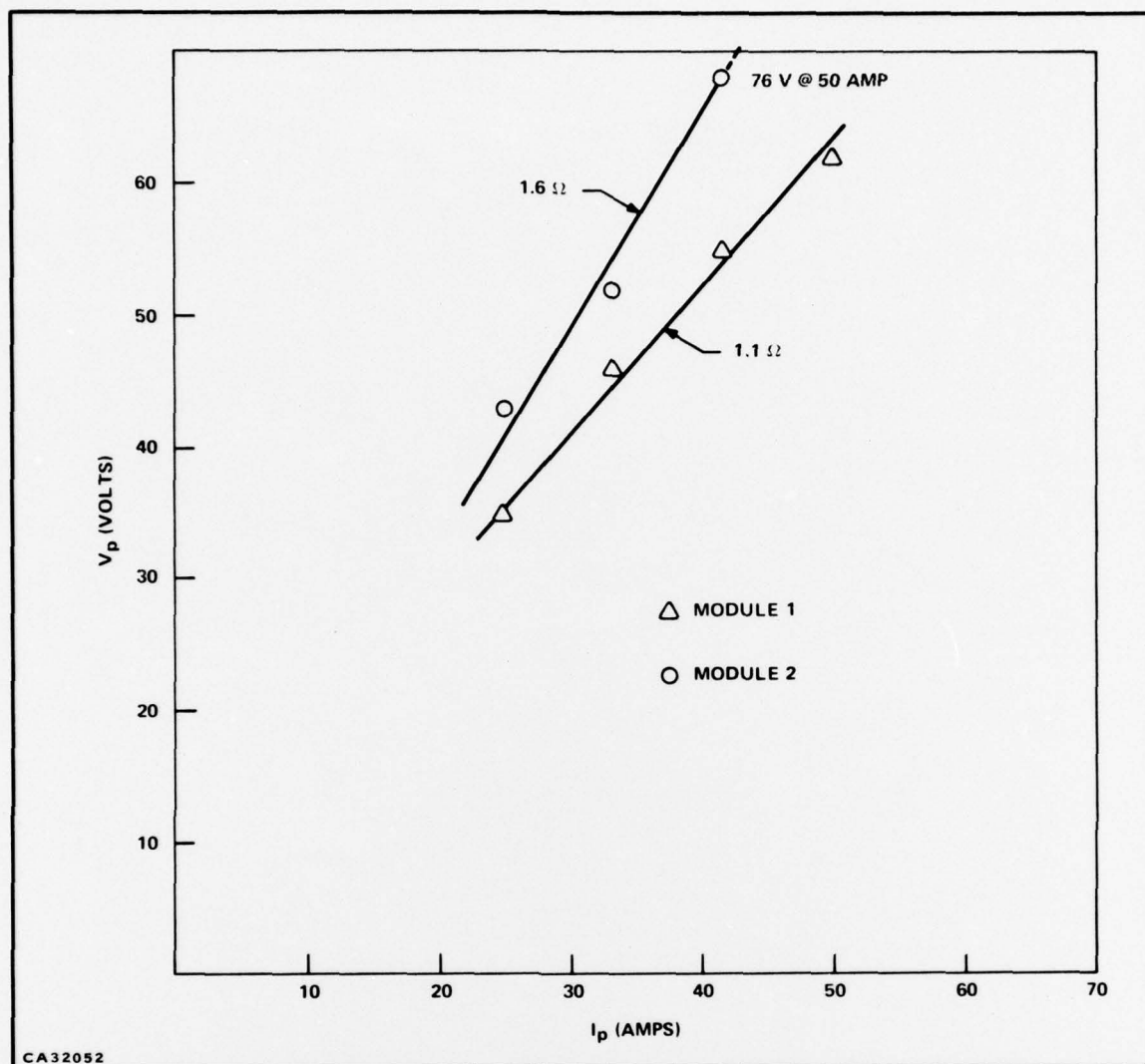
Figure 22. Peak Voltage versus Peak Current

Half-intensity beam solid-angle . . . . 38°
Power conversion efficiency at 50 amps, 150 ns, 100 Hz 1.5%
Power conversion efficiency at 50 amps, 150 ns, 5 kHz 1.25%
Emission aperture . . . . 15 mils by 20 mils
Number of diodes 18

31

SECTION V
SUMMARY

During this technical effort it was demonstrated that narrow-beam-angle large-optical-cavity 8500-Å wavelength injection lasers can be combined into an illuminator array and coupled optically to a small emission area using optical-fiber-ribbon light waveguides. Eighteen LOC laser diodes were connected in series electrically and coupled optically to an emission aperture of 15 mils by 20 mils.

The delivered array emitted 84 watts peak optical power at turn-on, or 62 watts after 2-minute operation, with a peak wavelength of 8420 Å, when driven by pulses of 50-amps peak current, 150-ns pulse width, and 5-kHz repetition rate.

Report No. 03-72-159

SECTION VI
REFERENCES

1.   H. Kressel et al., *Appl. Phys. Letters,* **Vol. 18, No. 2,** 15 January 1971, pp. 43-46.

2.   J. K. Butler and H. Kressel, IEEE Symposium on Injection Lasers, Boston, May 1972.

3.   J. K. Butler et al, *Appl. Phys. Letters,* **Vol. 17, No. 9,** p. 403 (1 November 1970).

4.   J. K. Butler, Quarterly Status Report No. 1, September 1971, Contract DAAK02-71-C-0263.

5.   J. K. Butler, Quarterly Status Report No. 2, November 1971, Contract DAAK02-71-C-0263.

6.   J. K. Butler, Quarterly Status Report No. 4, July 1972, Contract DAAK02-71-C-0263.

7.   D. T. F. Marple, *J. Applied Physics,* **35,** No. 4, April 1964, p. 1241.

8.   F. Stern, *Phys. Rev.,* **133,** 16 March 1964, p. A1653.

9.   Eugene Rocks, Technical Report AFAL-TR-71-307, p. 20.

APPENDIX

OPTICAL FIBERS

APPENDIX
OPTICAL FIBERS*

The fiber-optic ribbons used are composed of 12 1-by-1-mil-square fibers fused together in parallel (Figure A-1) to match the line source laser output.

Each fiber consists of a glass core of refractive index 1.57, surrounded by a glass cladding of index 1.48. Optical fibers transmit light by the phenomenon of total internal reflection. Light rays which strike the core/sheath interface at angles greater than the critical angle θ_c are reflected back into the core and travel to the other end of the fiber by a zigzag path of successive reflections.** The glass cladding is necessary to protect the core surface from contamination.

*The fibers used for this program were purchased from: Bendix Electro-Optics Division, Galileo Park, Sturbridge, Mass. 01518.
**N. S. Kapany, *Fiber Optics: Principles and Applications,* pp. 1-30, New York, Academic Press, 1967.
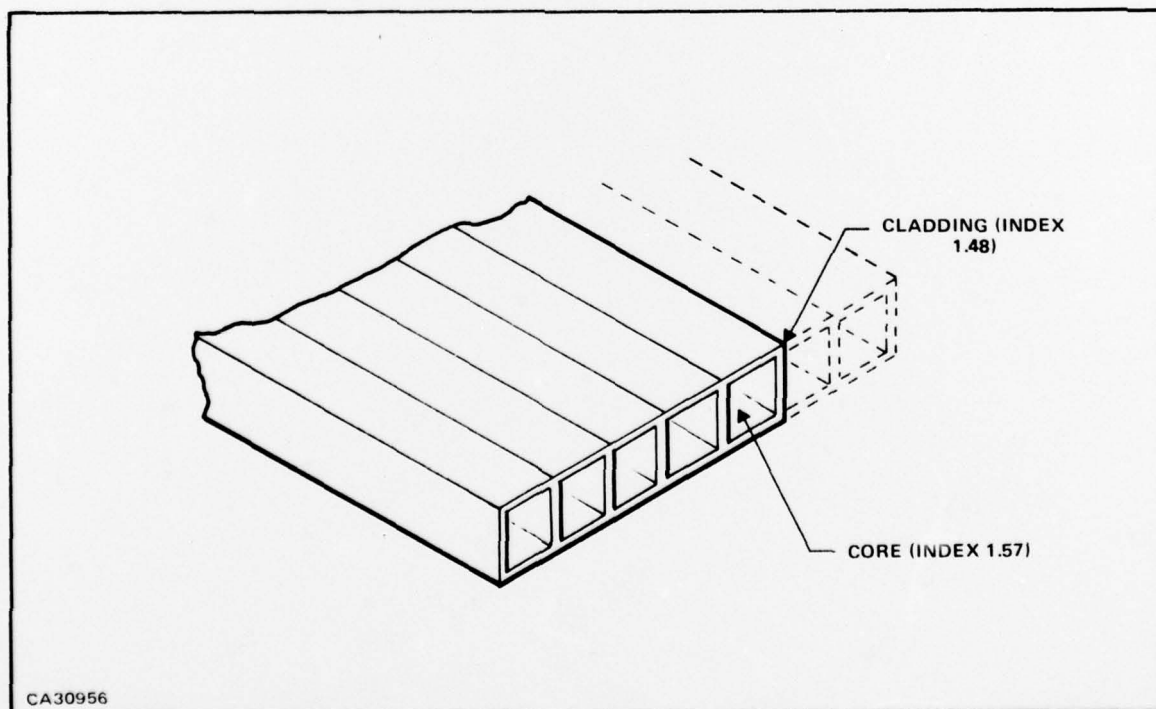

CLADDING (INDEX 1.48)

CORE (INDEX 1.57)

CA30956

Figure A-1. Fiber-Optic Ribbon (Individual, Square, Glass Fibers Fused Together)

For meridional rays, i.e., those that intersect the optical axis, Snell's law may be used to define a quantity called the numerical aperture, or NA, of the optical fiber. The NA is a measure of the maximum cone angle of light which the fiber can transmit. Figure A-2 shows the ray geometry.

$$NA = n_3 \sin \theta_{max} = (n_1^2 - n_2^2)^{1/2}$$

acceptance angle $= 2 \theta_{max}$.

For fiber of indices 1.57 and 1.48,

$$NA = 0.52$$

The f/number of the fiber is given by
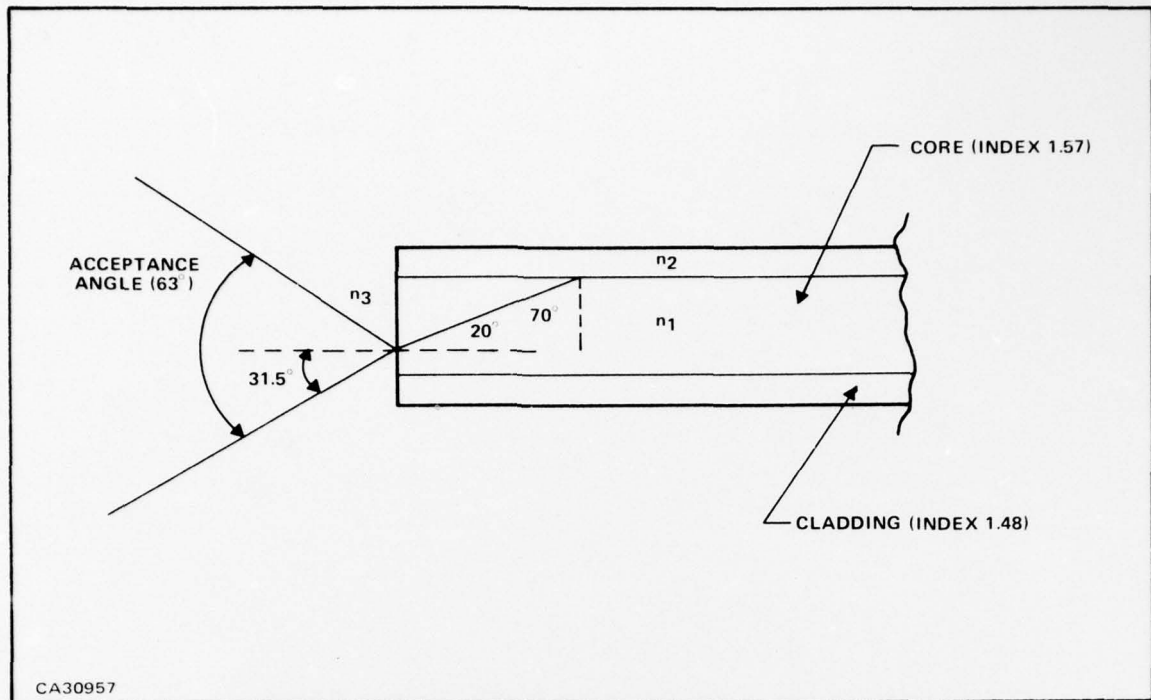
$$f/number = 1/(2NA) \cong 1.$$

Figure A-2. Diagram of Ray Passage Along an Optical Fiber (Rays Incident at the Fiber Wall at an Angle Greater than the Critical Angle are Trapped within the Fiber)

DOCUMENT CONTROL DATA - R & D

(Security classification of title, body of abstract and indexing annotation must be entered when the overall report is classified)

1. ORIGINATING ACTIVITY (Corporate author)	2a. REPORT SECURITY CLASSIFICATION
Texas Instruments Incorporated P. O. Box 5012 Dallas, Texas 75222	Unclassified
	2b. GROUP

3. REPORT TITLE

Fiber-Optic-Coupled LOC Injection-Laser Array for 8500Å Room-Temperature Emission

4. DESCRIPTIVE NOTES (Type of report and inclusive dates)

Final Report

(Angstroms)

5. AUTHOR(S) (First name, middle initial, last name)

David L. Carr and Friedrich H. Doerbeck

6. REPORT DATE	7a. TOTAL NO. OF PAGES	7b. NO. OF REFS
December 1972	47	9
8a. CONTRACT OR GRANT NO. DAAK02-72-C-0257	9a. ORIGINATOR'S REPORT NUMBER(S) TI-03-72-159	
b. PROJECT NO.		
c.	9b. OTHER REPORT NO(S) (Any other numbers that may be assigned this report)	
d.		

10. DISTRIBUTION STATEMENT

11. SUPPLEMENTARY NOTES	12. SPONSORING MILITARY ACTIVITY Night Vision Laboratory U. S. Army Electronics Command Ft. Belvoir, Va. 22060

13. ABSTRACT

The objective of this program was to fabricate a fiber-optic-coupled injection-laser array for the wavelength of 8500 Å at room temperature. The laser devices used are of the narrow-beam-angle large-optical-cavity (LOC) type. The array emitted 84 watts peak optical power from an emission aperture of 15 mils by 20 mils, with a peak wavelength of 8420 Å and a half-intensity beamwidth of 38°, when driven with pulses of 50-amps peak current, 150-ns duration, and 5-kHz repetition rate.

DD FORM 1 NOV 65 **1473**

14 KEY WORDS	LINK A		LINK B		LINK C	
	ROLE	WT	ROLE	WT	ROLE	WT